Phys. Chem. Glasses: Eur. J. Glass Sci. Technol. B, April 2007, 48 (2), 85–91

Diffusivity and solubility of water in silica glass in the temperature range 23–200°C

A. Zouine, O. Dersch, G. Walter & F. Rauch*[1]

Institut für Kernphysik, J.W.Goethe-Universität, Max-von-Laue-Str. 1, 60438 Frankfurt/Main, Germany

Manuscript received 2 July 2006
Revised version received 11 January 2007
Accepted 31 January 2007

The hydration process of silica glass was investigated by hydrothermal experiments at temperatures from 23°C to 200°C. Depth profiles of incorporated hydrogen were measured by using nuclear reaction analysis (NRA) techniques. Values of the effective water diffusivity deduced from the profiles could be described by the common Arrhenius relationship (activation energy E_H=(72·3±2) kJ/mol, pre-exponential factor D_{e0}=7·6×10^{-5} cm^2/s). Values of the effective water solubility, when normalised to a constant water vapour pressure P, were found to follow the Van't-Hoff relationship similar to the case of inert gas solubility (enthalpy of solution ΔH(W)=(−31·5±1) kJ/mol, pre-exponential factor W_0/P=1·2×10^{16} cm^{-3}/100 kPa). Diffusivity and solubility values for molecular water at 150°C and 200°C, obtained by combining NRA results and IR-spectroscopy results from the literature and the present work, were used to test the applicability of the diffusion reaction model of Doremus in the temperature range studied here. The diffusivity values were found to be compatible with model predictions based on results for higher temperatures whereas the solubility values were much larger than predicted.

1.Introduction

Because diffusion of water into silica glass affects many physical and chemical properties of the material, this hydration process has been investigated extensively. Experimental data on diffusivity and solubility for the temperature range 250°C to 1150°C were reported by Davis & Tomozawa.[1] Their paper also cites preceding studies, mostly performed at temperatures above 500°C, and summarises the results. Recently, additional data for 250°C were reported by Oehler & Tomozawa.[2] Concerning lower temperatures, Lanford *et al*[3] performed measurements at 90°C and Helmich & Rauch[4] obtained data for the range 200 to 100°C.

The first two studies[1,2] were done by using IR spectroscopy and thus could distinguish between the two water species, OH groups and molecular water; diffusion profiles were deduced using sample sectioning. These papers and, more comprehensively, Ref. 5 showed that below 350°C molecular water becomes significant beside OH, the clearly dominating species at high temperatures; earlier believe was that molecular water would occur only in silica glasses with total water contents much higher than used in the experiments of Refs 1, 2 and 5. In the studies by Lanford *et al*, and Helmich & Rauch, a nuclear reaction analysis (NRA) technique was employed to measure H diffusion profiles, using the fact that the appearance of H in the SiO_2 matrix is a signature for the incorporation of water. The two water species cannot be distinguished by this technique. An advantage of H profiling by NRA is the high depth resolution which permits the analysis of rather shallow diffusion profiles. Helmich & Rauch also performed hydration experiments with ^{18}O enriched water in the same temperature range and measured ^{18}O depth profiles by a NRA technique.[4]

In the theoretical treatment a widely used model of the diffusion process is the diffusion reaction model of Doremus.[6,7] References to alternative concepts are cited in Ref. 7; the paper by Behrens & Novak[8] is also of interest here. The model of Doremus assumes that water molecules in silica glass can be described essentially by analogy to physically dissolved inert gases. Thus, they populate voids in the SiO_2 network and are the diffusing species, transporting hydrogen and oxygen. An additional feature is that they can interact with the SiO_2 network by the (reversible) reaction

$$H_2O + SiOSi \leftrightarrow SiOH + HOSi \quad (1)$$

The OH groups formed in the reaction are assumed to be basically immobile. Results obtained by Helmich & Rauch[4] provide support for these assumptions. Concerning the concentration of dissolved water molecules, C, it should be proportional to that in the gas phase, C_g, and, hence, to the water vapour pressure, P; further, the ratio C/C_g should be of similar magnitude

[1]Corresponding author. Email f.rauch@em.uni-frankfurt.de
* Present address: Gesellschaft für Schwerionenforschung mbH, Planckstr. 1, 64219 Darmstadt, Germany

as for inert gases. By applying this model to diverse experimental diffusion data for temperatures above 300°C, Doremus obtained a coherent picture for the molecular water diffusivity in this range, with the diffusion coefficients following nicely the Arrhenius law.[7] We shall come back to this result in Section 4.

With regard to the concentration of OH groups, S, there is the empirical relation $S^2 \sim P$ for temperatures above 300°C. Together with the above assumption that $C \sim P$ this means that $S^2 \sim C$. The square root dependence implies that the two OH groups formed by the above reaction behave as independent entities, e.g. there is some OH diffusivity in this T range.[7] In contrast, for low temperatures it is expected[7] that the two OH groups stay paired for long times. Then the concentration of OH groups will be proportional to that of water molecules and, thus, to the water vapour pressure. This expectation has been confirmed experimentally. The relation $S \sim C$ was observed at 250°C for a wide concentration range,[2] and the ratio S/C was found to be nearly independent of P in measurements at 150 and 250°C.[5]

The aim of the present work has been to gain more complete data on water diffusivity and solubility for temperatures 200°C and below. This range will be called the low-T range hereafter. The low-T range is a relevant temperature range with respect to many practical uses of silica glass and likely of SiO_2 thin films, too.[3] It was also of interest to see if the successful application of the diffusion reaction model at high temperatures could be extended to the low-T range. Similar to before,[4] we employed NRA techniques for characterising the hydration layers formed in the samples by hydrothermal treatment. Additional information was gained by IR spectroscopy. In our previous study[4] we observed a time dependent H surface concentration, c_0. The time span to reach the equilibrium state of the above reaction, characterised by a saturation value of c_0, was between several hours and several days. In the present work this fact was taken into account: The data reported here were obtained in experiments for which the treatment times were chosen sufficiently long that equilibrium or near equilibrium was established. Time dependent surface concentrations of OH groups and molecular water have been reported also by the Tomozawa group.[1,2]

2. Experimental

2.1 Samples and hydrothermal treatments

The experiments were conducted with samples of the silica glass Infrasil 301 (a type-I fused quartz) purchased from Heraeus Quarzglas GmbH. According to the catalogue of the supplier, this glass has an overall metallic impurity content of typically 26 wt ppm and its intrinsic OH content is less than 8 wt ppm. When expressed in the units used in the present paper, this value of the intrinsic OH content represents an intrinsic H concentration value of $6{\cdot}2\times10^{17}$ cm^{-3}. (For silica glass, the conversion is 1 wt ppm OH to $7{\cdot}8\times10^{16}$ cm^{-3} H. The form chosen here for stating H concentration values seems preferable to the form wt ppm OH used in many papers because, as noted above, the NRA techniques cannot distinguish between the different water species.) Our NRA measurements of the intrinsic H concentration of this glass resulted in $1{\cdot}1\times10^{18}$ cm^{-3}, with an error of about 30%. This value is somewhat higher than to be expected from the quoted OH content; at any rate, the intrinsic H concentration could be neglected in the evaluation of the diffusion profiles.

The samples were in the form of flat plates with dimensions 1 mm×10 mm×10 mm. In order to obtain fresh surfaces they were etched in 10% HF for 10 min. For the hydrothermal treatments the samples were immersed in distilled water, either H_2O or D_2O, which was contained in (partly filled) teflon lined stainless steel vessels. The vessels were put in an oven set at the desired temperature, T. The T values ranged from 60°C to 200°C. They are listed in Table 1, as are the values of the treatment time, t. Since the vessels were closed the variation of the treatment temperature implied a variation of the water vapour pressure (see Table 1). In experiments at 23°C, one sample was kept in H_2O in a teflon container, under which condition P=2·8 kPa, and another sample was kept in the open atmosphere with mean relative humidity of 50%, corresponding to P=1·4 kPa. The samples were analysed by NRA usually a few days after the hydrothermal treatment. As shown before[4] the hydrogen profiles are very stable at room temperature.

2.2 Measurements

H depth profiles were measured by means of the ^{15}N technique that we have used before for this purpose.[4,9] It is based on the resonant nuclear reaction ^{1}H(^{15}N, $\alpha\gamma$)^{12}C. The sample is bombarded with ^{15}N ions. The reaction γ-ray yield is recorded as function of the stepwise increased ^{15}N energy (starting at the resonance energy 6·4 MeV) and is then converted into the H concentration as function of depth. More details may be found in Ref. 9. The depth range of this technique is about 2·5 μm. The ^{15}N ion beam was delivered by the 7 MV Van-de-Graaff accelerator of the Institut für Kernphysik.

For determining D depth profiles the nuclear reaction D(^{3}He,p)^{4}He was used.[10] In this technique one measures (at a fixed ^{3}He ion beam energy) the energy spectrum of the protons which is then converted into the D depth profile. The procedure is similar to that for determining ^{18}O profiles using the reaction ^{18}O(p, α)^{15}N.[4] The D profile measurements were done

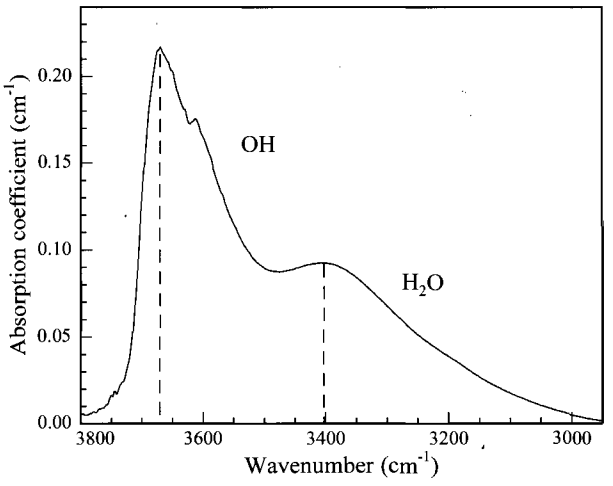

Figure 1. IR spectrum of a sample hydrated at 200°C for 1440 h, after subtracting the spectrum of an untreated sample. The OH band and the H_2O band appearing in the spectrum are discussed in the text

with 1·5 MeV ^{3}He ions at the 2 MV Van-de-Graaff accelerator of the Institut für Kernphysik. The depth range of this technique is 5 μm.

Two IR spectra were measured on a hydrated (H_2O; 200°C, 1440 h) and on an unhydrated sample, each of thickness 0·2 mm. The instrument used was a Nicolet spectrometer (Mod. IR 550) at the Gesellschaft für Schwerionenforschung, Darmstadt.

3. Results and discussion

Figure 1 shows the IR spectrum of the sample hydrated at 200°C for 1440 h, after subtracting the spectrum of the unhydrated sample. The two absorption bands with maxima at about 3670 cm^{-1} and at

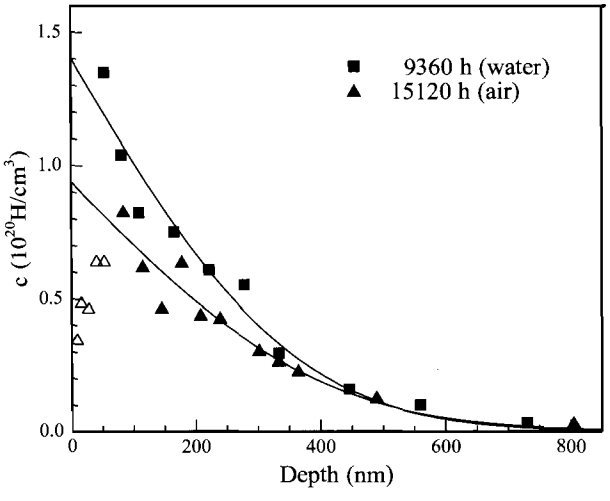

Figure 2. Hydrogen depth profiles of samples treated at 23°C. The lines through the data points are fit curves obtained by using Equation (2). The data points represented by the open symbol (Δ) were omitted in fitting the profile of the sample hydrated in air (compare text)

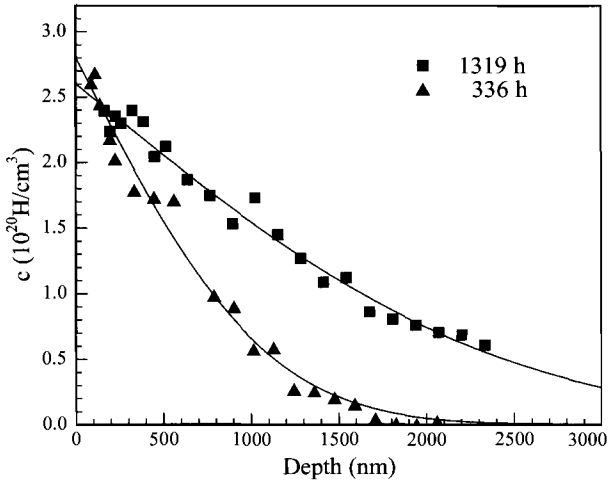

Figure 3. Hydrogen depth profiles of samples treated at 100°C. The lines through the data points are fit curves obtained by using Equation (2)

about 3400 cm^{-1} are the OH band and the H_2O band, respectively. As can be seen the H_2O band is relatively strong, signifying that an appreciable fraction of the incorporated water exists as water molecules. This observation is in accordance with the finding by the Tomozawa group mentioned in Section 1 about the increasing significance of this species at temperatures lower than 350°C.[1,2,5] In the discussion further below the ratio of the amplitudes of the OH band and the H_2O band obtained from Figure 1 will be exploited.

Several of the measured H and D depth profiles are displayed in Figures 2 to 4. The scatter of data points originates in statistical errors. The lines shown are fit curves obtained by using Equation (2)

$$c=c_0\mathrm{erfc}(x)/(2\sqrt{(D_e t)}) \qquad (2)$$

in which c is the H or D concentration, c_0 is the respective surface concentration, erfc is the complementary

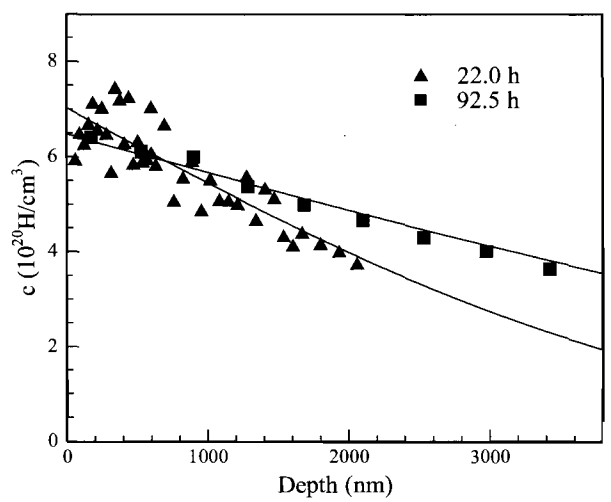

Figure 4. Hydrogen depth profiles of samples treated at 200°C. The lines through the data points are fit curves obtained by using Equation (2)

error function, t is the hydration time and D_e is the diffusion coefficient. This functional form (2) was found to describe all the profiles measured over their full range and, hence, it was used also for the remaining ones. In the 23°C/air profile the near surface data points lie lower than to be expected. The reason for this is not clear. However, it seemed justified to omit these data points in fitting the profile.

It should be noted that D_e is an effective diffusion coefficient for water (in the form of OH groups and of water molecules), which is to be distinguished from the diffusion coefficient for water molecules mentioned in Section 1. This point will be discussed further below. Also the concentration of hydrogen relates to both species and may be expressed as the sum $c=2C+S$, where the factor 2 accounts for the two hydrogen atoms of the water molecule. Specifically, for the surface concentration the relation is $c_0=2C_0+S_0$.

The D_e and c_0 values obtained are listed in Table 1. (For the convenience of readers accustomed to units wt ppm OH, two H concentration values are given into these units; the c_0 value in the first line corresponds to $1{\cdot}0\times10^3$ wt ppm OH, the one in the last line corresponds to $5{\cdot}4\times10^3$ wt ppm OH). The errors of the D_e values are 20–30%; in some cases, when the profiles could not be measured over the full depth, they are about 30%. The errors of the c_0 values are between 15% and 20%. Within the error limits, the D_e and c_0 values from samples treated in H_2O agree with those from samples treated under the same conditions in D_2O. Therefore, they will not be distinguished henceforth, and the letter H will denote both hydrogen isotopes. This agreement is in line with the diffusion mechanism: The diffusivity ratio of the two kinds of molecules, given by the square root of the mass ratio D_2O/H_2O, is only 5%.

Table 1. Treatment conditions and results from the evaluation of H (D) profiles

T (°C)	P (*kPa*)	t (*h*)	I (*a*)	D_e (cm^2/s)	c_0 (10^{20} cm^{-3})
23	2·8	9360	H	$1{\cdot}2\times10^{-17}$	1·4
	1·4	15120	H	$9{\cdot}0\times10^{-18}$	0·9
60	19·9	1416	H	$2{\cdot}9\times10^{-16}$	1·9
		2136	D	$3{\cdot}4\times10^{-16}$	1·8
70	31·2	744	H	$2{\cdot}1\times10^{-15}$	2·5
80	47·3	1416	H	$1{\cdot}2\times10^{-15}$	2·5
100	101	336	H	$2{\cdot}9\times10^{-15}$	2·8
		1319	H	$3{\cdot}7\times10^{-15}$	2·6
120	199	168	D	$2{\cdot}6\times10^{-14}$	3·3
140	361	253	D	$5{\cdot}8\times10^{-14}$	3·8
		1147	D	$1{\cdot}0\times10^{-13}$	3·8
150	476	336	H	$1{\cdot}2\times10^{-13}$	3·7
		336	D	$1{\cdot}1\times10^{-13}$	3·7
160	618	112	H	$6{\cdot}2\times10^{-14}$	5·0
170	792	408	D	$1{\cdot}6\times10^{-13}$	5·3
200	1554	22	H	$7{\cdot}7\times10^{-13}$	6·9
		45	H	$8{\cdot}5\times10^{-13}$	7·3
		92·5	D	$6{\cdot}0\times10^{-13}$	6·3

(a) H and D stand for hydrothermal treatment in H_2O and D_2O, respectively.

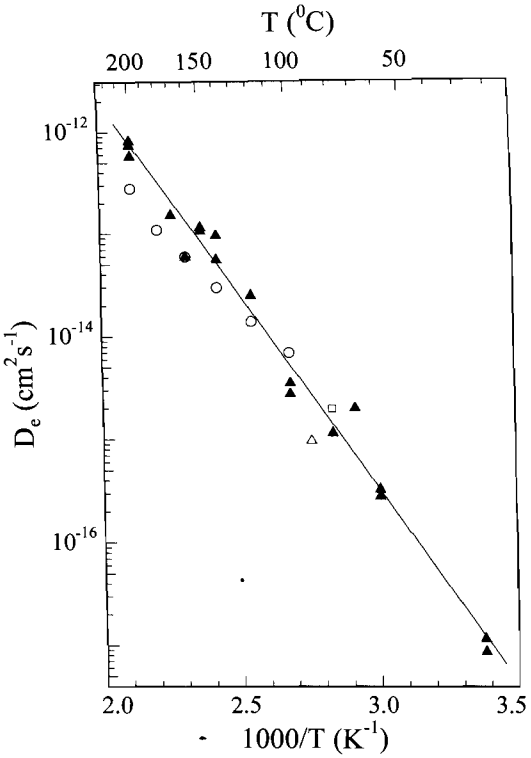

Figure 5. Arrhenius diagram showing the values of the effective diffusion coefficients D_e obtained in the present work (symbol: ▲). The line is a least squares fit to these D_e values. Also shown are D_e values from previous studies, as discussed in the text. Those from Ref. 4 are represented by the symbol ○, the D_e value from Ref. 3 by the symbol Δ and the D_e value from Ref. 1 by the symbol □

Table 1 shows that the c_0 values at 200°C found for treatment times from 22 h to 92·5 h agree well among each other. As noted in Section 1, this means that equilibrium has been reached for t=22 h (or perhaps somewhat shorter times). The mean value $c_0=6{\cdot}8\times10^{20}$ cm^{-3} also agrees closely with the c_0 value found in Ref. 4 after 6 days. The c_0 values for two different t values agree also at 140°C, at 100°C and at 60°C. Since, in general, the treatment times chosen in the experiments increased with decreasing temperature in order to make up for the decreasing reaction rate, we believe that equilibrium or near-equilibrium was attained in all cases. The t values for 160 and 120°C are relatively short. However, the corresponding c_0 values fit well into the systematic trend of the other c_0 values (see Figure 7). Thus, it is justified to take all the surface concentration values c_0 as saturation values. This means that also $2C_0$ and S_0 are saturation values.

The D_e values will be discussed first. They cover about five orders of magnitude as a function of temperature. This dependence is visualised in the Arrhenius diagram of Figure 5. In setting up the diagram we presumed that the D_e values do not depend on the pressure P during the hydrothermal

treatment. This supposition seems well justified in view of the small compressibility coefficients of silica glass ($2{\cdot}6\times10^{-11}$/Pa[11]) and of the void size of silica glass ($1{\cdot}8\times10^{-10}$/Pa[12]). As Figure 5 shows, the set of D_e values can be well described by the relationship

$$D_e(T)=D_{e0}\exp(-E_H/RT) \quad (3)$$

where D_{e0} is the pre-exponential factor, E_H is the activation energy, T is the absolute temperature and R is the gas constant. A least squares fit through the data points, denoted as the Arrhenius line, hereafter, results in E_H=(72·3±2) kJ/mol and $D_{e0}=7{\cdot}6\times10^{-5}$ cm^2/s ($\log D_{e0}=-4{\cdot}12\pm0{\cdot}32$).

There are some experimental results from previous studies which can be compared to the present ones (compare Figure 5). The D_e values obtained by Helmich & Rauch[4] for T=100–200°C are compatible with the values found here, taking into account the error ranges. The activation energy derived from those D_e values, 55±7 kJ/mol, is to be superseded by the new, better founded value. The D_e value at 90°C obtained by Lanford *et al*,[3] 1×10^{-15} cm^2/s, is somewhat low compared to the present results. In Ref. 1, Figure 17, a D_e value for OH groups at T=80°C is reported which amounts to about 2×10^{-15} cm^2/s as may be read from this figure. It agrees fairly well with the present D_e value at 80°C. Such agreement between the D_e values for H and for OH is in accordance with the relation S~C that holds in the low-T range, see Section 1.

The relationship (3), together with the value of the activation energy, describes the effective diffusivity of water in the temperature range covered. This kind of information is valuable with regard to practical uses of silica glass. Of interest regarding the model description are diffusion coefficients for molecular water, D_{mw}. At equilibrium, where S~C holds, D_{mw} is connected with D_e by the relation[13]

$$D_{mw}=D_e\times(1+S/(2C)) \quad (4)$$

(The factor 2 takes into account that two OH groups are formed by the conversion of one water molecule.) The ratio S/C is accessible through IR spectra; it closely corresponds to the absorbance ratio of hydroxyl band and water band since the molar absorptivities ε for the two bands are nearly equal numerically, 77·5 $l_{glass}/mol_{OH}cm_{glass}$ and 81 $l_{glass}/mol_{H_2O}cm_{glass}$.[5] From the IR spectrum in Figure 1 one finds $S/C\approx2{\cdot}3$ at 200°C and from IR spectra at 150°C[1,5] one finds $S/C\approx1{\cdot}3$. The resulting D_{mw} values, calculated by using the respective mean D_e values in Equation (4), are $1{\cdot}6\times10^{-12}$ cm^2/s and $1{\cdot}9\times10^{-13}$ cm^2/s, respectively. At this point, it may be noted that the quantity S/C decreases with decreasing temperature. This becomes evident when the above S/C values are considered together with those obtainable from IR spectra at 250°C, where $S/C\approx3{\cdot}0$[2] and ≈2·5,[5] and at 300°C, where $S/C\approx3{\cdot}5$.[14] (The shapes of the OH and H_2O bands in the various IR spectra differ somewhat; thus, it is expedient to take the absorbance ratios only as approximate values.)

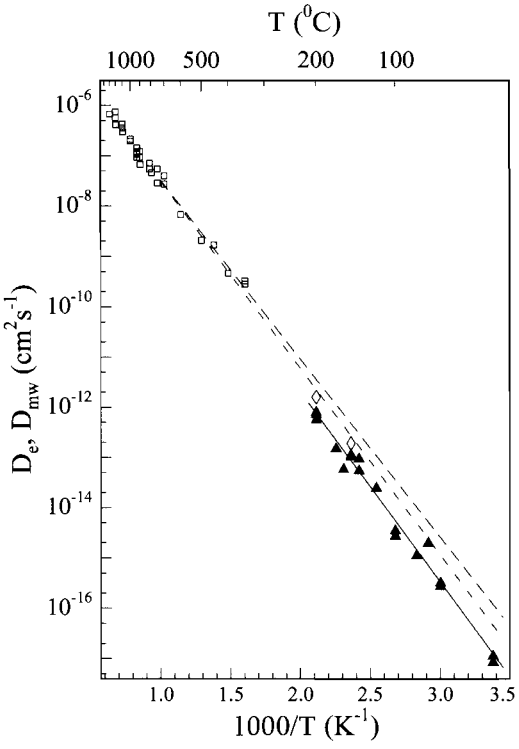

Figure 6. Arrhenius diagram showing the same D_e values as in Figure 5 (symbol: ▲) and in addition the two D_{mw} values obtained in the present work (symbol: ◊); further, D_{mw} values taken from Ref. 7 are shown, compare text (symbol: □). The full line is a least squares fit to the D_e values, as in Figure 5. The dashed line is a least squares fit to the D_{mw} values from Ref. 7. The dashed-dotted line is a least squares fit to the D_{mw} values from Ref. 7 and from the present work

With the two D_{mw} values gained here the applicability of the diffusion reaction model in the range below 350°C can be assessed, starting from the expectation that, as in the case of inert gases,[15] one single activation energy E_{mw} will describe the molecular water diffusivity for the entire range from room temperature to high temperatures. The Arrhenius diagram of Figure 6 shows in the lower right part the present D_e data, as in Figure 5, and in addition the two D_{mw} values calculated above; in the upper left part are shown the D_{mw} values calculated by Doremus[7] which were referred to in Section 1. (They are listed in Tables I, III and IV of Ref. 7.) These values had been derived from experimental D_e values for OH and ^{18}O in the temperature range 1300 to 350°C; the ratio C/C_g appearing in the derivation had been 0·015, as suggested by results for inert gases.[7] The dashed line in Figure 6 results from a least squares fit to these data that we have carried out; the corresponding activation energy is E_{mw}=(67·9±1) kJ/mol. (Ref. 7 states that the activation energy "is about 70 kJ/mol".)

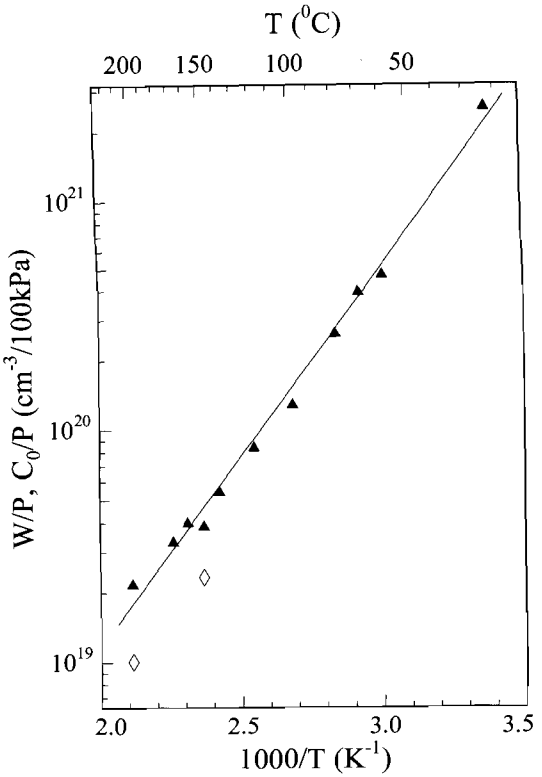

Figure 7. Van't Hoff diagram showing the values of W/P *(symbol: ▲), the total water solubility normalised to pressure, as obtained in the present work. The line is a least squares fit to the* W/P *values. Also shown are two values of* C_0/P *(symbol: ◊), the molecular water solubility normalised to pressure, calculated as described in the text*

As can be seen, the fit line runs rather close to the two D_{mw} data points obtained in the present study. This proximity gives support to the assumptions used in the calculation of the D_{mw} values of Ref. 7. We deemed it justified, consequently, to add the two low lying D_{mw} values to those from Ref. 7 for attaining an improved Arrhenius line for molecular water diffusion. The result of the least squares fit to this expanded data set is shown in Figure 6 as a dashed-dotted line. The respective activation energy is (71·2±1) kJ/mol ($\log D_{mw0}$=−3·78±0·06).

Compared to the dashed line this Arrhenius line is better compatible with the present D_e data and with the temperature trend of S/C described above. This trend would call for a slope still a little larger, a condition that may be achieved, e.g. if in the model calculation for the range 1300°C to 350°C the ratio C_0/C_g employed is changed slightly or allowed to slowly vary with temperature. Additional S/C data for temperatures below 150°C could provide a more quantitative basis. At any rate, the above E_{mw} value as well as one somewhat larger than 71·2 kJ/mol fits well into the sequence of activation energies of inert gases as function of the molecular radius.[15]

We now turn to the concentration values and related quantities. It was noted above that c_0, C_0 and S_0 are saturation values. Since the saturation value represents the solubility at the respective temperature and pressure, C_0 and S_0 represent the molecular water solubility and the "solubility" of OH groups. Thence, the sum $C_0+S_0/2$ corresponds to the total (or effective) water solubility. In the following, this quantity will be denoted W; numerically, W is half the surface concentration c_0.

The values of the total water solubility vary by less than a factor 10 (compare the c_0 values in Table 1), quite different from the case of the D_e values. Since C and S both are proportional to the water vapor pressure P and this variable changes by more than a factor 500, the small variation means that the solubility strongly decreases with increasing temperature. For visualising the temperature dependency, the total solubility data normalised to a constant pressure of 100 kPa are shown in Figure 7 in a Van't-Hoff-type diagram, in analogy to the treatment of solubility data for Ar[16] and for Ne.[17] (In the cases of two or three W values at a given temperature, the mean value has been employed.) The data set is well described by the relationship

$$W/P=(W_0/P)\exp(-\Delta H(W)/RT) \qquad (5)$$

in which W_0/P is the pre-exponential factor and $\Delta H(W)$ is the enthalpy of solution. A least squares fit results in the values $\Delta H(W)$=(−31·5±1) kJ/mol and W_0/P=1·2×10^{16} cm^{-3}/100 kPa ($\log(W_0/P)$=−16·08±0·13). Thus, there is a coherent description of the effective water solubility as function of temperature and pressure that should be valuable for applications of silica glass in the temperature range investigated.

Some conclusions can be drawn also with regard to molecular water solubility. By using the above values for S/C at 200°C and 150°C, the solubility values C_0/P for these temperatures are obtained, amounting to 46% and 60% of the associated W/P values. They have been plotted in Figure 7. It appears reasonable to assume that C_0/P has the same functional dependency on temperature as W/P. For the associated enthalpy of solution, $\Delta H(C_0)$, an approximate value range can be gained by utilising the trend of S/C noted above. This trend implicates that the difference between W and C_0 decreases with decreasing temperature. Therefore, $\Delta H(W)$ may be taken as one margin of the value range. A rough estimate for the other margin should be provided by the slope of the line defined by the C_0/P data point at 200°C and a virtual data point at 23°C, defined by assuming that $S_0 \ll C_0$ at this temperature, i.e. $C_0(23°C) \approx W(23°C)$. The slope corresponds to about 36 kJ/mol, so that the approximate value range for $\Delta H(C_0)$ is −31 to −36 kJ/mol. This value range compares fairly well with the enthalpies of solution for Ar and Ne in silica glass, 31·5 kJ/mol[16] and 6·7 kJ/mol,[17] respectively. Thus, with respect to this quantity dissolved molecular water is compara-

ble to inert gases.

The absolute solubility values for molecular water are about $1{\cdot}6\times10^{20}$ cm^{-3} at 200°C and about $1{\cdot}1\times10^{20}$ cm^{-3} at 150°C. These values are well compatible with the concentration of voids, about 10^{21} cm^{-3}, that are accessible to inert gases of the size of water molecules.[15] It must be noted, however, that they are much larger than the values corresponding to the relation $C/C_g \approx 0{\cdot}015$ which holds for inert gases as well as for molecular water at high temperatures (see above). When expressed in this form, one obtains $C/C_g \approx 0{\cdot}7$ and $\approx 1{\cdot}4$ at 200°C and 150°C, respectively; at 23°C this ratio is 62 if S/C does not decrease further than the 150°C value, otherwise it will be even larger. When considered in the framework of the Doremus model, the relatively large C/C_g values found indicate that only some small fraction of the water molecules is in an unbound state like that of inert gases while the other fraction is in a state not included in the model. This inference is in qualitative agreement with the finding by Davis & Tomozawa[5] that the water band in the IR spectra of silica glass hydrated at low temperatures consists of three components; one of them is attributed to free, unbound water molecules and two others to hydrogen bonded and structurally bound water molecules.

4. Summary

The present work provides for the first time a rather complete set of data on the effective water diffusivity and solubility in silica glass for the temperature range below 200°C. It is found that even at such low temperatures the contact of silica glass with water or humidity affects the glass to a significant degree. At room temperature a surface layer of several 100 nm becomes hydrated in the course of several months and the H concentration reaches a value of about 1×10^{20} cm^{-3} (equivalent to about $0{\cdot}9\times10^3$ wt ppm OH), a rather high impurity level. These new data should be helpful in assessing the behaviour of silica glass during treatment steps and with regard to long term performance. Of scientific interest are the results on the diffusivity and solubility of molecular water in silica glass. The diffusivity results largely corroborate the assumption of the diffusion reaction model of Doremus that molecular water behaves similar as inert gases; however, the solubility values found disagree with the model predictions and indicate that water molecules are dissolved also in other forms.

References

1. Davis, K. M. & Tomozawa, M. Water diffusion in silica glass: structural changes in silica glass and their effect on water solubility and diffusivity. *J. Non-Cryst. Solids*, 1995, **185**, 203–220.
2. Oehler, A. & Tomozawa, M. Water diffusion into silica glass at low temperature under high water pressure. *J. Non-Cryst. Solids*, 2004, **347**, 211–219.
3. Lanford, W. A., Burman, C. & Doremus, R. H. Diffusion of water in SiO_2 at low temperatures. In: R. L. Snyder, R. A. Condrate, Sr & P. F. Johnson (eds.): *Materials Science Research, Vol. 19*. New York, London: Plenum Press 1985, p. 203–208.
4. Helmich, M. & Rauch, F. On the mechanism of diffusion of water in silica glass. *Glastech. Ber.*, 1993, **66**, 195–200.
5. Davis, K. M. & Tomozawa, M. An infrared spectroscopic study of water-related species in silica glasses. *J. Non-Cryst. Solids*, 1996, **201**, 177–198.
6. Doremus, R. H. The diffusion of water in fused silica. In: *Reactivity of Solids.*, eds J. W. Mitchell, R. W. Roberts & P. Cannon, Wiley, New York, 1969, p.667.
7. Doremus, R. H. Diffusion of water in silica glass. *J. Mater. Res.*, 1995, **10**, 2379–2389.
8. Behrens, H. & Novak, M. The mechanism of water diffusion in polymerized silicate melts. *Contrib. Mineral. Petrol.*, 1997, **126**, 377–385.
9. March, P. & Rauch, F. Leaching studies of soda-lime-silica glass using deuterium- and ^{18}O-enriched solutions. *Glastech. Ber.*, 1990, **63** (6), 154–162.
10. Pronko, P. P. & Pronko, J. G. Depth profiling of ^3He and ^2H in solids using the $^3He(d,p)^2H$ resonance, *Phys. Rev.*, 1974, **B9**, 2870–2878.
11. Brückner, R. Silicon Dioxide. In: *Encyclopedia of Applied Physics, Vol. 18*. VHC Publishers, Inc., 1997.
12. Hugenschmidt, C. & Maier, K. Pressure dependence of the void size in silica studied by positron annihilation. *Mater. Sci. Forum*, 1997, **255–257**, 469–471.
13. Crank, J. *Mathematics of diffusion*. Second edition, Oxford Press, London, 1975.
14. Wakabayashi, H. & Tomozawa, J. Diffusion of water into silica glass at low temperature. *J. Am. Ceram. Soc.*, 1989, **72**, 1850–1855.
15. Doremus, R. H. *Glass Science*, Second edition, Wiley, 1994.
16. Nakayama, G. S. & Shackelford, J. F. Solubility and diffusivity of argon in vitreous silica. *J. Non-Cryst. Solids*, 1990, **126**, 249–254.
17. Wortman, R. S. & Shackelford, J. F. Gas transport in vitreous silica fibers. *J. Non-Cryst. Solids*, 1990, **125**, 280–286.